

Highlights

Electric Double Layer at the Metal-Oxide/Electrolyte Interface

Lisanne Knijff, Mei Jia, Chao Zhang

- Introduces the physical chemistry of the protonic double layer at the metal-oxide/electrolyte interface.
- Summarizes ways of determining the double-layer capacitance and the potential from experimental methods.
- Discusses the atomistic modelling of the protonic double-layer, with an emphasis on the density-functional theory-based molecular dynamics simulations.

Electric Double Layer at the Metal-Oxide/Electrolyte Interface

Lisanne Knijff^a, Mei Jia^b, Chao Zhang^a

^a*Department of Chemistry-Ångström Laboratory, Uppsala University, Lägerhyddsvägen 1, BOX 538, Uppsala, 75121, Sweden*

^b*Henan Key Laboratory of Biomolecular Recognition and Sensing, Henan Joint International Research Laboratory of Chemo/Biosensing and Early Diagnosis of Major Diseases, College of Chemistry and Chemical Engineering, Shangqiu Normal University, Suiyang District, Shangqiu, 476000, China*

Abstract

Metal-oxide surfaces act as both Brønsted acids and bases, which allows the exchange of protons with the electrolyte solution and generates either positive or negative proton charges depending on the environmental pH. These interfacial proton charges are then compensated by counter-ions from the electrolyte solution, which leads to the formation of the electric double layer (EDL). Because the EDL plays a crucial role in electrochemistry, geochemistry and colloid science, understanding the structure-property relationship of the EDL in metal-oxide systems from both experimental and theoretical approaches is necessary. This chapter focuses on the physical chemistry of the protonic double layer at the metal-oxide/electrolyte interface. In particular, determinations of the EDL capacitance and the double-layer potential from potentiometric titration experiments, electrochemical methods, surface-sensitive vibrational spectroscopy and X-ray photoelectron spectroscopy are summarized. This is followed by discussions from the atomistic modelling aspect of the EDL, with an emphasis on the density-functional theory-based molecular dynamics simulations. A conclusion and outlook for future works on this topic are also given.

Keywords: metal oxide, surface charge, double layer, capacitance, density-functional theory, molecular dynamics

Email address: chao.zhang@kemi.uu.se (Chao Zhang)

1. Introduction

What we are going to face in the 21st century is an increase of the world-wide energy consumption by about 100% over the current level in the year of 2050¹. The corresponding yearly carbon emissions could reach about 75 gigatons by that time². The explosion of energy needs and the experience of extreme climates in recent years suggest that we are indeed at a crossroad. Therefore, energy and environment are the two outstanding challenges that our society is facing.

One promising solution towards these challenges is to use metal oxide-based materials. Metal oxides are a class of inorganic materials that have various energy and environmental applications such as heterogeneous catalysts, fuel cells, lithium-ion batteries, supercapacitors, water treatment and antimicrobial application^{3,4,5,6,7,8,9}. Metal-oxide surfaces are terminated by O²⁻ anions, the size of which is generally larger than that of the Mⁿ⁺ cations, and this results in a lower coordination of surface metal cations with respect to the bulk and their accessibility to reactive environments.

Most metal oxides are synthesized as nanostructures with different morphology and porosity, which leads to unique properties and reduced economical costs. For example, porous RuO₂ provides a very high specific capacitance of 1200 F g⁻¹ for supercapacitor applications due to the large surface area, the significant pore volume, and the high acid site concentration¹⁰. On the other hand, the very properties that make metal oxide nanostructures attractive and indispensable in modern science and technology also cause an issue for the environment and human safety. There have been increasing concerns about the release of spent metal oxide nanostructures (e.g. ZnO nanoparticles as the most toxic one) into the aquatic environments via wastewater discharge¹¹.

In both the functioning and the degradation of metal oxide nanostructures, the aqueous interface plays a vital role¹². The pH condition in which the surface has no net proton charge is called the point of zero charge. Since working conditions (acid and alkaline solutions) for most metal oxides are not at the point of zero charge¹³, aqueous interfaces of metal oxide are highly electrified due to the acid-base chemistry and a protonic double layer is formed by attracting counter-ions from the electrolyte solution. The formation of these protonic double layers is a general phenomenon observed for all insulating main group oxides, such as silicates and aluminates as well as the conducting oxides formed by transition metal oxides. Compared to

the metal/electrolyte interface, the surface charge density in these compact protonic double layers at the aqueous interface of oxides can be an order of magnitude larger¹⁴. Therefore, understanding the unique relationship between the protonic double-layer structure and the interfacial reactivity is a crucial step for designing metal oxide-based nanostructures. In the following, we will discuss the fundamentals of the protonic double layer from both experimental and theoretical aspects.

2. Acid-base Chemistry and the Point of Zero Charge

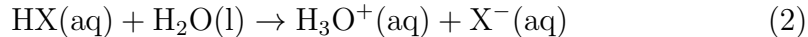
Acid-base reactions are a fundamental part of the metal-oxide chemistry, as they play an important role in the reactivity, the selectivity, and the formation of the protonic double layer. The idea of acid and base goes back to the 17th century where a base was seen as an anti-acid that can be made to react with an acid to form a salt. The modern understanding of the topic starts with Arrhenius (1884) who defined an acid as a compound that produces protons H^+ in aqueous solution and a base as a compound that produces hydroxyl ions OH^- in aqueous solution. Later, the unique role of protons was highlighted by Brønsted (1923)¹⁵ and Lowry (1923)¹⁶, which laid the foundation for the acid-base chemistry.

In Brønsted-Lowry acid-base theory, an acid is defined as a proton-donor and a base is defined as a proton-acceptor, i.e.



This means that one can define acid-base pairs, where amphiprotic molecules belong to multiple acid-base pairs. It is also important to note that Eq. 1 implies that there is always at least one ion-pair in an acid-base reaction, which entails the importance of electrostatic interactions in the determination of acidity.

To introduce the acidity or the pK_a , let us assume that the reaction that is being studied is:



Then, the corresponding reaction free energy ΔG is

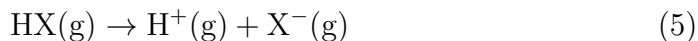
$$\Delta G = 2.30RT (pK_a - pK_{a,H_3O^+}) \quad (3)$$

where

$$pK_a = -\log(K_a) = -\log\left(\frac{[\text{H}^+][\text{X}^-]}{[\text{HX}]}\right) \quad (4)$$

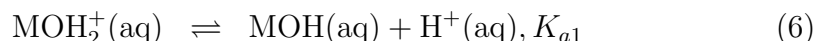
In the Brønsted scale, $pK_{a,\text{H}_3\text{O}^+} = -1.74$. Therefore, the significance of Eq. 2 is that it recasts the problem of determining the pK_a value into the free energy calculation of the proton transfer reaction, which is computationally feasible.¹⁷

Before moving on to surface acidity, it is worth mentioning a related quantity called proton affinity, which is defined as the enthalpy change for the following reaction:



When compared with Eq. 2, it is clear that the proton affinity is a gas-phase quantity whereas the pK_a value depends on the solvent.

Since metal oxides contain a wide variety of surface sites behaving as Brønsted acids and bases, reactions constantly occur when the surface comes into contact with an aqueous solution. The water molecules dissociate into protons and hydroxyl groups which strongly bind to the oxygen and metal atoms in the metal-oxide surface. Therefore, the pK_a of a metal-oxide surface is commonly defined around the surface hydroxyls which are written here as MOH. Here the M is a metal atom, and the OH is the hydroxyl group bound to it. This hydroxyl group can act as an acid or a base by donating or adsorbing a proton respectively. The corresponding deprotonation reactions are as follows:



Inspecting Eq. 6 and 7, it is clear that the surface charge of the metal oxide depends on the concentration of H^+ , or the pH of the aqueous solution.

When the surface bears no net proton charge, the concentrations of MOH_2^+ and MO^- will be equal. This means K_{a1} and K_{a2} would hold for the following expression:

$$K_{a1}K_{a2} = [\text{H}^+]_{\text{pzc}}^2 \quad (8)$$

Therefore, the corresponding pH for the neutral surface is

$$\text{pH}_{\text{pzc}} = -\log[\text{H}^+]_{\text{pzc}} = \frac{pK_{a1} + pK_{a2}}{2} \quad (9)$$

This is the so-called the point of zero charge (PZC). Fig. 1 presents a schematic diagram illustrating the manner in which the surface charge changes with pH.

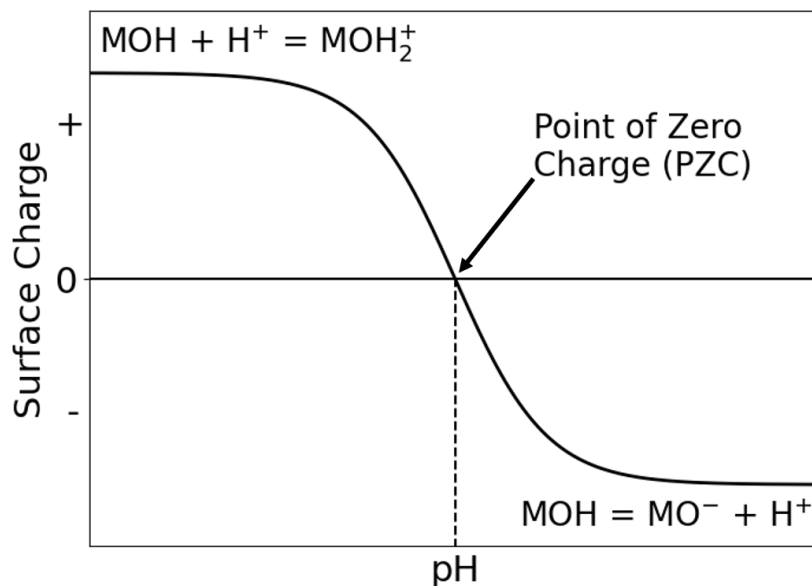


Figure 1: The point of zero charge at the metal-oxide/electrolyte interface.

For metal-oxides, there are several physical parameters that determine the PZC. Such parameters, for example, are the cation electronegativity, the cation ionic radius and its formal charge. The oxygen partial charge, and the surface site coordination also play an important role. However, their direct link is hard to describe using theory and thus mainly relies on empirical models.¹⁸

In the literature, the PZC and the isoelectric point (IEP) are sometimes used interchangeably. However, they are quite different quantities in nature because the referred charges are different. The PZC refers to the surface charge, while the IEP refers to the diffuse charge in the double layer.¹⁹ This leads us to the discussion of the double-layer structure at the metal-oxide/electrolyte interface as outlined in the next section.

3. The Formation of Electric Double Layer

The electric double layer (EDL) manifests itself at both the metal/electrolyte and the metal-oxide/electrolyte interfaces. The EDL at the metal/electrolyte

interface is a central topic in electrochemistry²⁰, while the EDL at the metal-oxide/electrolyte interface plays a crucial role in geochemistry and colloid science²¹.

Similar to the electrified metal surface, adsorption of ions at the metal-oxide/electrolyte interface leads to the formation of the EDL, which is schematically represented in Fig. 2. The first layer of the double layer consists of a layer of solvent molecules and ions that are directly adsorbed to the electrified surface. The ions that are part of this so-called inner Helmholtz layer, no longer have their full solvation shell intact and the average position of those ions corresponds to the inner Helmholtz plane (IHP). Then, ions that still have their full solvation shell are not able to get as close to the electrified surface. The average position of those ions is called the outer Helmholtz plane (OHP). Finally, the long-range electrostatic interactions of the electrolyte with the electrified interface lead to the formation of a whole concentration profile of solvated ions over a large distance. This is called the diffuse layer or the Gouy-Chapman layer, and reaches from the outer Helmholtz plane all the way to the bulk of the electrolyte.²² Despite of these great similarities between the EDL at the metal/electrolyte interface and that at the metal-oxide/electrolyte interface, there are also significant differences in several aspects.

The first difference between the EDL at the metal-oxide/electrolyte interface as compared to that at the metal/electrolyte interface is the charging mechanism. The excess charge at the metal surface is due to the rearrangement of the electronic density under an external perturbation (e.g. a voltage source). In contrast, the excess charge at the metal-oxide surface is generated by acid-base chemistry, as discussed in the previous section. Apart from these acid/base interactions, other reactions occur as well. Since it is possible for some of the metal ions to dissolve in the electrolyte solution because of the pH condition, these can then react with deprotonated surface hydroxyls to form surface complexes instead. Moreover, these reactions happen exactly within the Helmholtz layer, which would alter the Helmholtz capacitance considerably. Nevertheless, it is worth noting that the distinction between the electronic charge versus the proton charge may not be clear-cut. For conducting oxides, such as RuO_2 , both electronic charge and proton charge can exist simultaneously. In addition, most metal surfaces will be oxidized at a higher potential. Therefore, a combination of both charging mechanisms is more of a rule than an exception.

The second difference comes from the addition of the space-charge (SC)

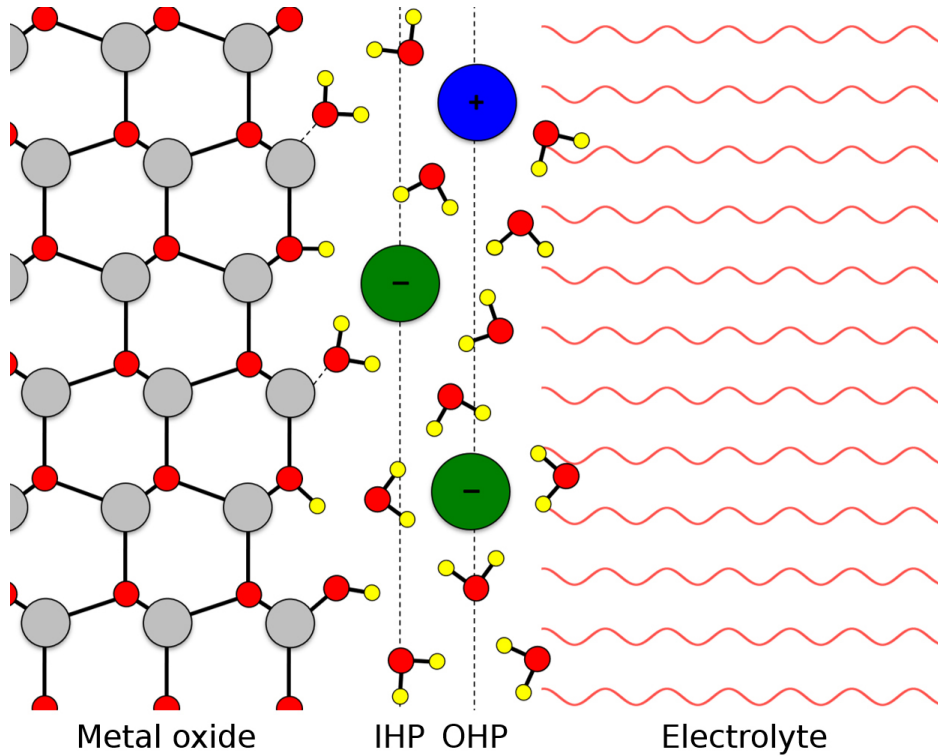


Figure 2: Model for the double layer region at the metal-oxide/electrolyte interface IHP, inner Helmholtz plane; OHP, and outer Helmholtz plane.

layer in metal-oxides. The space-charge layer is a result of the fact that metal-oxides have a much lower electronic conductivity, and less free electrons in general. Because of that, charging at the surface can no longer instantaneously be compensated, and instead leads to the depletion or accumulation of electrons at the metal-oxide surface. The layer where this is the case is referred to as the SC layer, which can have a thickness of 10-100 nm.²²

The electrostatic potential difference at the interface with respect to that in the bulk of the semiconductor is $\Delta\phi_{SC}$. In the case of an n -type semiconducting oxide, the concentration of electrons in the conduction band is enhanced when $\Delta\phi_{SC}$ is positive. Vice versa, the concentration of electrons at the surface is reduced (and that of holes increased) when $\Delta\phi_{SC}$ is negative, as shown in Fig. 3. The situations of p -type semiconducting oxides are simply the opposite. Note that the band bends downwards ($\Delta\phi_{SC} > 0$) and upwards ($\Delta\phi_{SC} < 0$) depending on the sign of $\Delta\phi_{SC}$, and that the potential

at which $\Delta\phi_{\text{SC}} \approx 0$ is called the flat-band potential.

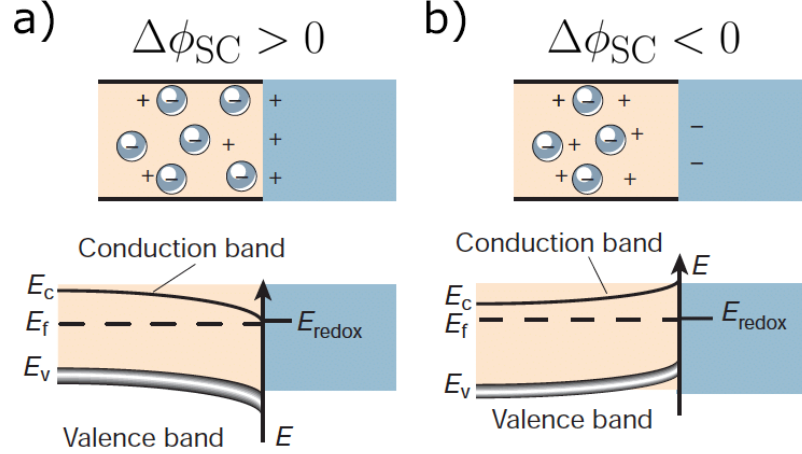


Figure 3: The *n*-type semiconductor/electrolyte interface. a) Accumulation layer causes downward bending of the conduction and valence bands. b) Depletion layer causes upward bending of the conduction and valence bands. Adapted from Ref.²³ with permission (Copyright 2019 the Springer Nature Group)

Taking these factors into consideration, this means that the capacitance of a metal-oxide/electrolyte interface consists of three components, i.e. the capacitance of the space-charge layer C_{SC} , the capacitance of the Helmholtz layer C_{H} and the capacitance of the Gouy-Chapman layer C_{GC} , as follows:

$$\frac{1}{C_{\text{EDL}}} = \frac{1}{C_{\text{SC}}} + \frac{1}{C_{\text{H}}} + \frac{1}{C_{\text{GC}}} \quad (10)$$

The capacitance of the space-charge layer is similar to that of the Gouy-Chapman layer in the electrolyte. They are analogous, where the electrons in the space-charge layer can be seen as the ions in the Gouy-Chapman layer. Therefore, the expression for the capacitance can be obtained in a similar fashion by solving the one-dimensional Poisson-Boltzmann equation. This results in the so-called Mott-Schottky relation:

$$\frac{1}{C_{\text{SC}}^2} = \left(\frac{2L_D}{\epsilon\epsilon_0} \right)^2 \left(\frac{e\Delta\phi_{\text{SC}}}{kT} - 1 \right) \quad (11)$$

where ϵ is the dielectric constant, ϵ_0 is the vacuum permittivity, k is the Boltzmann factor and T is the temperature. L_D therein is the Debye

length at a given concentration of the bulk electron concentration n_0 with the following expression

$$L_D = \left(\frac{\epsilon\epsilon_0 kT}{2n_0 e^2} \right)^{1/2} \quad (12)$$

Compared to the space-charge layer and the Gouy-Chapman layer, the Helmholtz layer involves both short-range and long-range interactions. This makes it an indispensable factor that affects the chemical reactivity at the electrified metal-oxide/electrolyte interface. Moreover, C_H is also the dominating term in Eq. 10 at a high salt concentration and the flat potential condition ($\Delta\phi_{SC} = kT/e$). Therefore, we will see how C_H can be determined from both experimental and computational methods in the following sections.

4. Double-layer Capacitance and Potential from Experiments

The most used technique for determining the surface charge and the double layer capacitance at metal-oxide/electrolyte interfaces is the potentiometric titration method.

In potentiometric titration experiments, the surface charge density σ_0 is determined from the surface concentrations Γ_{H^+} and Γ_{OH^-} of H^+ and OH^- species respectively, as

$$\sigma_0 = F(\Gamma_{H^+} - \Gamma_{OH^-}) \quad (13)$$

The surface concentration Γ therein is measured from the volume change $\Delta v = v_b - v_d$ of the titrant added to the solution before and after the dispersion of metal oxide nanoparticles at a constant pH condition, as illustrated in Fig. 4. Note that the specific surface area is needed in the conversion from Δv to Γ , which is either assumed a priori or measured by separate experiments²⁴.

Subsequently, the capacitance can be obtained via the following formula²⁵:

$$C = \frac{d\sigma_0}{d\psi} = \frac{Fd(\Gamma_{H^+} - \Gamma_{OH^-})}{2.30RTd\text{pH}} \quad (14)$$

For semi-conducting oxides, impedance spectroscopy, which measures the resistive response to a time-varying electric field²⁶, can also be applied. The impedance, as the ratio between the input voltage and the output current, has a real and imaginary components, which are directly related to the frequency-dependent conductivity and capacitance. These components are commonly

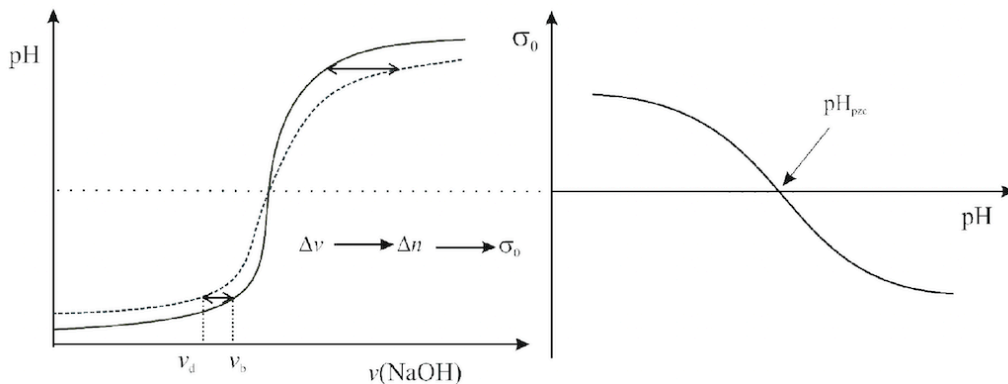


Figure 4: Schematic representation of the potentiometric titrations (left) of a colloid suspension (dashed line) and a blank titration without colloid particles (full line) and the resulting proton related surface charge density (right) as a function of pH. Adapted from Ref.²⁴ under the terms of CC-BY licence (Copyright 2012 Authors).

represented in a complex plane as the so-called Nyquist plot. Then, equivalent circuit models are used to separate the contributions from the double layer and the space-charge layer to the overall capacitance²⁷.

For conducting oxides, such as RuO_2 , cyclic voltammetry can also be used, in which the current response is recorded with respect to a linear potential sweep²⁸. Since the potential increases (or decreases) linearly with time in cyclic voltammetry, the corresponding surface charge can be calculated by integrating the current. Thus, the $I - V$ curve can be readily converted to $dQ/dV - V$ curve, which shows the potential-dependence of the capacitance²⁹. However, it should be pointed out that the capacitance obtained in this way is usually attributed as the pseudo-capacitance, which is a result of surface redox reactions.

In addition to the titration and electrochemical methods mentioned above, surface-sensitive vibrational spectroscopy and X-ray photoelectron spectroscopy can also be used to probe the double-layer potential in the Helmholtz layer. They distinguish themselves from electrokinetic techniques that measure the zeta potential (the diffuse-layer potential).

In the second harmonic generation (SHG)/sum-frequency generation (SFG) method, the polarization response is zero for any centro-symmetric environments, which makes the technique interface-selective. Then, the polarization at electrified metal-oxide/electrolyte interfaces contains the contributions

from both the second-order susceptibility $\chi^{(2)}$ and the third-order susceptibility $\chi^{(3)}$ ^{30,31}.

$$P_{2\omega} = \chi^{(2)}E_{\omega}E_{\omega} + \chi^{(3)}\Delta\phi_{\text{EDL}}E_{\omega}E_{\omega} \quad (15)$$

The second-order susceptibility $\chi^{(2)}$ couples to the interfacial water and the surface hydroxyl groups in the frequency of O-H stretching, while the third-order susceptibility $\chi^{(3)}$ is related to the double-layer potential $\Delta\Phi_{\text{EDL}}$. Therefore, $\Delta\phi_{\text{EDL}}$ can be measured at a given pH condition from SHG/SFG experiments and the surface pK_a can be determined accordingly.

In X-ray photoelectron spectroscopy, high-energy X-rays are used to probe the sample, which can cause electrons to be ejected from the probed species. The kinetic energy of those electrons can then be used to determine the binding energy (BE) of the electron in the same material. Therefore, the change in BE of metal-oxide nanoparticles at a given pH with respect to the PZC gives access to the double-layer potential^{32,33}.

$$\text{BE} - \text{BE}_{\text{PZC}} = e\Delta\phi_{\text{EDL}} \quad (16)$$

Subtracting the zeta potential due to the diffuse layer and incorporating the surface charge density measured from the potentiometric titration experiment, this provides another means to estimate the double-layer capacitance of the Helmholtz layer.

5. Atomistic Modelling of the Protonic Double Layer

Modelling of the protonic double layer at the metal-oxide/electrolyte interface started around the 1960s by relating the PZC with the formal ionic charge of the cation, and its ionic radius³⁴. There, it was found that basic oxides consist of cations with a low formal charge. High formal charges on the other hand result in acidic oxides. This emphasizes again the important role of the electrostatic interaction in the metal-oxide systems and triggered the development of surface complexation models (SCMs) from the 1970s^{35,36,37,38}. Among those, the multisite complexation model (MUSIC)³⁹ and its charge-distribution variant (CD-MUSIC)⁴⁰ are most notable ones. In the MUSIC model, the phenomenological surface sites are taken into account to describe the adsorption and desorption of protons following the 2-pK model shown in Eqs. 6 and 7, and the surface charges upon protonation/deprotonation are determined using the Pauling bond valence model (i.e. the charge of the

metal cation is divided by the number of coordinating groups). Later, it was extended in the CD-MUSIC model, where the charge of the inner-sphere complexes in the double layer is distributed over the surface plane and the next electrostatic plane in order to match the macroscopic adsorption data. In these models, the double layer is treated as a series of parallel-plate capacitors for adjusting the surface concentration of ions.

Despite that the MUSIC and the CD-MUSIC model have been successfully applied to study different oxide materials such as silica, hematite, cerium oxide, rutile and anatase among others⁴¹, it is worth noting that the binding constant (for proton adsorption/desorption), the Helmholtz capacitance and the pK_a value are fitting parameters to reproduce the potentiometric titration data. This raises questions about the physical soundness of surface complexation modelling⁴². Moreover, SCMs are purely thermodynamic models, the surface heterogeneity and the temporal evolution of the double layer are simply out of reach. This calls for atomistic modelling, which can provide predictive structural, dynamical and energetic information.

In particular, density-functional theory-based molecular dynamics (DFTMD) simulations^{43,44} are in principle well-suited for modelling the protonic double layer, where the distinction between reactive solutes and solvent has all but disappeared. In DFTMD, the force on the atom is computed “on-the-fly” by solving the electronic Schrödinger equation during the time evolution of the system. Therefore, bond forming/breaking, electronic polarization and charge transfer effects are all included. This is in contrast with MD simulations based on classical force fields^{45,46}, in which the parameters used in predefined functional forms to describe the bonded and non-bonded interactions are obtained by fitting either structural and spectroscopic data of simple hydrated compounds or quantum chemical calculations^{47,48,49}.

While DFTMD can be highly accurate, it is also computationally very demanding. This makes DFTMD simulations of the electrified solid-liquid interface seemingly impractical. However, endeavours have been attempted to address this challenging problem^{50,51,52,53}, and breakthroughs have recently been made by the development of finite-field DFTMD⁵⁴.

Since periodic boundary conditions are applied to the simulation cell (also known as the supercell), there are naturally two choices for setting up the protonic double layer in a DFTMD simulation. In the symmetric setup, two sides of the metal-oxide slab bear the same amount and the same type of proton charge and there is no supercell dipole in the overall system. Instead, in the asymmetric setup, two sides of the metal-oxide slab take the same

amount but opposite types of proton charge and this leads to a net polarization in the system. The symmetric setup for the DFTMD modelling of the protonic double layer has been applied to systems of $\text{TiO}_2(110)/\text{NaCl}$ solution⁵⁰ and hematite/ NaF solution⁵¹. Cheng and Sprik showed that the double-layer charging has a significant effect on the structure of the rutile $\text{TiO}_2(110)/\text{water}$ interface using DFTMD, as the water molecules are forced to align their dipoles with the electric field. Values found for the capacitance are lower by a factor of 3 than the experimental value of $100 \mu\text{F cm}^{-2}$, although there is also a large uncertainty in the experimental estimation⁵⁰. Similarly, Ulman et al. adopted the symmetric setup in their DFTMD simulations of the hematite/ NaF electrolyte interface and found that for the hydroxylated surface the value of the Helmholtz capacitance is about $40.3 \mu\text{F cm}^{-2}$ while it changes to $51 \mu\text{F cm}^{-2}$ for the FeO_3Fe termination⁵¹.

Compared to the symmetric setup of the supercell, the asymmetric setup has the merit that the chemical composition is kept fixed when changing the surface charge density and the supercell dipole P_z becomes a new observable from the simulation. This motivated the development of finite-field DFTMD by exploring the constant electric displacement \bar{D} Hamiltonian⁵⁵. It has been shown that constant \bar{D} simulation significantly speeds up the convergence of the supercell polarization and it also provides a more accurate calculation for the Helmholtz capacitance C_H , as the finite-size error due to the application of periodic boundary conditions is removed⁵⁶. In this setup, the Helmholtz capacitance C_H can be readily obtained from the supercell polarization P_z using the following expression:

$$C_H = \frac{1}{2\pi L_z} \left(\frac{\partial \sigma_0}{\partial \langle P_z \rangle} \right)_{\bar{D}} \quad (17)$$

where L_z is the supercell length in the direction in which \bar{D} field is applied and σ_0 is the surface proton-charge density.

The first study of the protonic double layer using the finite-field DFTMD approach was carried out for the rutile $\text{TiO}_2(110)/\text{NaCl}$ electrolyte interface (Fig. 5a). As shown by Zhang et al.⁵², the supercell polarization converges quickly by switching the electric boundary condition from constant \bar{E} to constant \bar{D} (Fig. 5 b). Moreover, a stronger fluctuation of the water molecules is found at a higher pH as compared to that at a lower pH (Fig. 5 c), which leads to a 50% increase in the Helmholtz capacitance from about $60 \mu\text{F cm}^{-2}$ to $90 \mu\text{F cm}^{-2}$. It is also found that What contributes to the Helmholtz

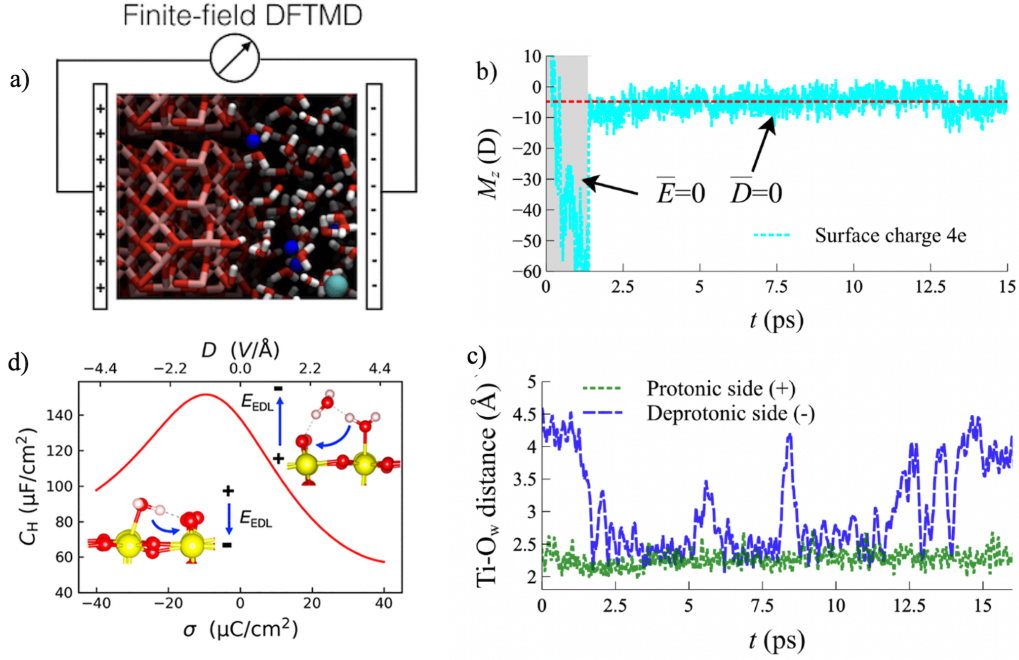


Figure 5: a) An illustration of the finite-field DFTMD applied to the rutile $\text{TiO}_2(110)/\text{NaCl}$ electrolyte interface; b) The effect of the electric boundary condition on the time evolution of the supercell polarization; c) The water dynamics at the electrified interface of the rutile $\text{TiO}_2(110)$; d) The differential Helmholtz capacitance resolved from the finite-field DFTMD simulation. Adapted from Ref.⁵² with permission (Copyright 2019 American Chemical Society) and Ref.⁵³ under the terms of CC-BY licence (Copyright 2021 Authors).

capacitance is the proton exchange between the surface group and the solvating water molecules. When both adsorbed water molecules and charged surface groups are constrained to not undergo reaction, C_H becomes quite close to the previous results⁵⁰. These findings highlight the importance of the dynamical description in the modelling of the protonic double layer.

Subsequently, finite-field DFTMD has also been applied to study SnO_2 , which is an isostructure of TiO_2 and has a characteristic dissociative water adsorption⁵⁷. Jia et al.⁵³ computed the Helmholtz capacitance of the $\text{SnO}_2(110)/\text{NaCl}$ electrolyte interface and developed a differential Helmholtz capacitance model accordingly. It is found that Dissociative adsorption of water at the surface leads to a higher Helmholtz capacitance ($109 \mu\text{F cm}^{-2}$) when compared to the molecular adsorption of water ($61 \mu\text{F cm}^{-2}$). More

importantly, it is shown that the dipole at the interface changes the double layer potential significantly and the specific orientation of chemisorbed water molecules leads to an asymmetric profile of the differential Helmholtz capacitance (Fig. 5 d). This explains the molecular origin for asymmetric EDLs seen experimentally in a range of metal oxides/hydroxides.

6. Conclusion and Outlook

In this chapter, we summarize the fundamentals of the protonic double layer formed at the metal-oxide/electrolyte interface, and discuss the current understanding and the recent progress on this topic from both experimental and theoretical approaches.

Nevertheless, given the importance of metal-oxide surfaces in practical applications, our understanding of the relationship between the EDL structure and the chemical reactivity is still quite limited. This may not come as a total surprise for an interdisciplinary area where colloid science, electrochemistry and surface science overlap. On one hand, most knowledge of protonic EDL is based on macroscopic observations such as current and concentration from colloid science and electrochemistry, as discussed in this chapter. On the other hand, surface science studies which provided great microscopic insight into various types of surface defects (e.g., oxygen vacancies and surface reconstruction) and surface reactions were mostly performed in ultra-high vacuum (UHV) conditions^{58,59,60}. In this regard, recent advances in experimental techniques such as high-resolution scanning tunnelling microscopy⁶¹, atomic force microscopy⁶² and apparatus for dosing liquid water in UHV conditions⁶³ are quite promising to study EDLs at the metal-oxide/electrolyte interface and to bridge this knowledge gap.

Complement to these experimental advances, materials modelling approaches, in particular, finite-field DFTMD simulations have been successfully applied to investigate structure and reactivity of EDLs at the metal-oxide/electrolyte interface, as discussed in this chapter. Further investigations to disentangle the signals from the surface-sensitive vibrational spectroscopy at charged oxide surfaces would be interesting^{64,65}. Nevertheless, many processes associated with EDLs, e.g. the dissolution of the metal-oxide surface and the charging dynamics, cannot possibly be described with a few hundred atoms and tens of picoseconds typically provided by DFTMD. Therefore, data-driven approaches such as atomistic machine learning could be transformative here for modelling the metal-oxide/electrolyte interface⁶⁶,

as it allows for large-scale simulations with the accuracy of reference electronic structure calculations but only at a fraction of the computational cost⁶⁷.

References

- [1] US Energy Information Administration, Annual Energy Outlook. 2019.
- [2] OECE, OECD Environmental Outlook to 2050. 2011.
- [3] Ardizzone, S.; Trasatti, S. Interfacial properties of oxides with technological impact in electrochemistry. *Adv. Colloid Interface Sci.* **1996**, *64*, 173 – 251.
- [4] Winter, M.; Brodd, R. J. What are batteries, fuel cells, and supercapacitors? *Chem. Rev.* **2004**, *104*, 4245 – 4270.
- [5] Simon, P.; Gogotsi, Y. Materials for electrochemical capacitors. *Nat. Mater.* **2008**, *7*, 845 – 854.
- [6] Song, F.; Bai, L.; Moysiadou, A.; Lee, S.; Hu, C.; Liardet, L.; Hu, X. Transition metal oxides as electrocatalysts for the oxygen evolution reaction in alkaline solutions: An application-inspired renaissance. *J. Am. Chem. Soc.* **2018**, *140*, 7748–7759.
- [7] Ren, Y.; Ma, Z.; Bruce, P. G. Ordered mesoporous metal oxides: Synthesis and applications. *Chem. Soc. Rev.* **2012**, *41*.
- [8] Zheng, M.; Tang, H.; Li, L.; Hu, Q.; Zhang, L.; Xue, H.; Pang, H. Hierarchically nanostructured transition metal oxides for lithium-ion batteries. *Adv. Sci.* **2018**, *5*, 1700592 – 24.
- [9] Raghunath, A.; Perumal, E. Metal oxide nanoparticles as antimicrobial agents: A promise for the future. *Int. J. Antimicrob. Agents* **2017**, *49*, 137 – 152.
- [10] Lokhande, C.; Dubal, D.; Joo, O.-S. Metal oxide thin film based supercapacitors. *Curr. Appl. Phys.* **2011**, *11*, 255–270.
- [11] Joo, S. H.; Zhao, D. Environmental dynamics of metal oxide nanoparticles in heterogeneous systems: A review. *J. Hazard. Mater.* **2017**, *322*, 29–47.

- [12] Mu, R.; Zhao, Z.-j.; Dohnálek, Z.; Gong, J. Structural motifs of water on metal oxide surfaces. *Chem. Soc. Rev.* **2017**, *46*, 1785–1806.
- [13] Lyons, M. E. G.; Doyle, R. L.; Browne, M. P.; Godwin, I. J.; Rovetta, A. A. S. Recent developments in electrochemical water oxidation. *Curr. Opin. Electrochem.* **2017**, *1*, 40 – 45.
- [14] Sato, N. *Electrochemistry at metal and semiconductor electrodes*; Elsevier: Amsterdam, 1998.
- [15] Brønsted, J. N. Einige Bemerkungen über den Begriff der Säuren und Basen. *Recl. Trav. Chim. Pays-Bas* **1923**, *42*, 718–728.
- [16] Lowry, T. M. The uniqueness of hydrogen. *J. Soc. Chem. Ind.* **1923**, *42*, 43–47.
- [17] Cheng, J.; Liu, X.; VandeVondele, J.; Sulpizi, M.; Sprik, M. Redox potentials and acidity constants from density functional theory based molecular dynamics. *Acc. Chem. Res.* **2014**, *47*, 3522 – 3529.
- [18] Noguera, C. *Physics and chemistry at oxide surfaces*; Cambridge University Press, 1996.
- [19] Lyklema, J. *Fundamentals of interface and colloid science: Soft colloids*; Elsevier, 2005; Vol. 5.
- [20] Schmickler, W.; Santos, E. *Interfacial electrochemistry*; Springer Science & Business Media, 2010.
- [21] Bunker, B. C.; Casey, W. H. *The aqueous chemistry of oxides*; Oxford University Press, 2020.
- [22] Memming, R. *Semiconductor electrochemistry*; John Wiley & Sons, 2015.
- [23] Grätzel, M. Photoelectrochemical cells. *Nature* **2001**, *414*, 338–344.
- [24] Lützenkirchen, J.; Preočanin, T.; Kovačević, D.; Tomišić, V.; Lövgren, L.; Kallay, N. Potentiometric titrations as a tool for surface charge determination. *Croat. Chem. Acta* **2012**, *85*, 391 – 417.

- [25] Bérubé, Y. G.; De Bruyn, P. L. Adsorption at the rutile-solution interface. II. Model of the electrochemical double layer. *J. Colloid Interface Sci.* **1968**, *28*, 92–105.
- [26] Lvovich, V. F. *Impedance spectroscopy: Applications to electrochemical and dielectric phenomena*; Wiley, 2012.
- [27] Tomkiewicz, M. The potential distribution at the TiO₂ aqueous electrolyte interface. *J. Electrochem. Soc.* **1979**, *126*, 1505 – 1510.
- [28] Faulkner, L. R.; Bard, A. J. *Electrochemical methods: Fundamentals and applications*; John Wiley and Sons, 2002.
- [29] Sugimoto, W.; Yokoshima, K.; Murakami, Y.; Takasu, Y. Charge storage mechanism of nanostructured anhydrous and hydrous ruthenium-based oxides. *Electrochim. Acta* **2006**, *52*, 1742–1748.
- [30] Ong, S.; Zhao, X.; Eissenthal, K. B. Polarization of water molecules at a charged interface: Second harmonic studies of the silica/water interface. *Chem. Phys. Lett.* **1992**, *191*, 327–335.
- [31] Bischoff, M.; Biriukov, D.; Předota, M.; Roke, S.; Marchioro, A. Surface potential and interfacial water order at the amorphous TiO₂ nanoparticle/aqueous interface. *J. Phys. Chem. C* **2020**, *124*, 10961–10974.
- [32] Brown, M. A.; Abbas, Z.; Kleibert, A.; Green, R. G.; Goel, A.; May, . S.; Squires, T. M. Determination of surface potential and electrical double-layer structure at the aqueous electrolyte-nanoparticle interface. *Phys. Rev. X* **2016**, *6*, 011007 – 12.
- [33] Brown, M. A.; Goel, A.; Abbas, Z. Effect of electrolyte concentration on the Stern layer thickness at a charged interface. *Angew. Chem. Int. Ed.* **2016**, *128*, 3854 – 3858.
- [34] Parks, G. A. The isoelectric points of solid oxides, solid hydroxides, and aqueous hydroxo complex systems. *Chem. Rev.* **1965**, *65*, 177–198.
- [35] Schindler, P.; Kamber, H. R. Die Acidität von Silanolgruppen. Vorläufige Mittheilung. *Helv. Chim. Acta* **1968**, *51*, 1781–1786.

- [36] Stumm, W.; Huang, C. P.; Jenkins, S. R. Specific chemical interaction affecting the stability of dispersed systems. *Croat. Chem. Acta* **1970**, *42*, 223 – 244.
- [37] Davis, J. A.; James, R. O.; Leckie, J. O. Surface ionization and complexation at the oxide/water interface: I. Computation of electrical double layer properties in simple electrolytes. *J. Colloid Interface Sci.* **1978**, *63*, 480 – 499.
- [38] Westall, J.; Hohl, H. A comparison of electrostatic models for the oxide/solution interface. *Adv. Colloid Interface Sci.* **1980**, *12*, 265–294.
- [39] Hiemstra, T.; Riemsdijk, W. v.; Bolt, G. Multisite proton adsorption modeling at the solid/solution interface of (hydr)oxides: A new approach I. Model description and evaluation of intrinsic reaction constants. *J. Colloid Interface Sci* **1989**, *133*, 91–104.
- [40] Hiemstra, T.; van Riemsdijk, W. H. A surface structural approach to ion adsorption: The charge distribution (CD) model. *Journal of colloid and interface science* **1996**, *179*, 488–508.
- [41] Brown Jr, G. E.; Parks, G. A. Sorption of trace elements on mineral surfaces: Modern perspectives from spectroscopic studies, and comments on sorption in the marine environment. *Int. Geol. Rev.* **2001**, *43*, 963–1073.
- [42] Bickmore, B.; Rosso, K.; Mitchell, S. In *Surface Complexation Modelling*; Lützenkirchen, J., Ed.; Elsevier, 2006; Chapter 9, pp 269–283.
- [43] Car, R.; Parrinello, M. Unified approach for molecular dynamics and density-functional theory. *Phys. Rev. Lett.* **1985**, *55*, 2471 – 2474.
- [44] Marx, D.; Hutter, J. *Ab initio molecular dynamics: Basic theory and advanced methods*; Cambridge University Press, 2012.
- [45] Předota, M.; Bandura, A. V.; Cummings, P. T.; Kubicki, J. D.; Wesolowski, D. J.; Chialvo, A. A.; Machesky, M. L. Electric double layer at the rutile (110) surface. 1. Structure of surfaces and interfacial water from molecular dynamics by use of ab initio potentials. *J. Phys. Chem. B* **2004**, *108*, 12049 – 12060.

- [46] Perez, S.; Přeboda, M.; Machesky, M. Dielectric properties of water at rutile and graphite surfaces: Effect of molecular structure. *J. Phys. Chem. C* **2014**, *118*, 4818 – 4834.
- [47] Bandura, A. V.; Kubicki, J. D. Derivation of force field parameters for TiO₂-H₂O systems from ab initio calculations. *J. Phys. Chem. B* **2003**, *107*, 11072 – 11081.
- [48] Cygan, R. T.; Liang, J.-J.; Kalinichev, A. G. Molecular models of hydroxide, oxyhydroxide, and clay phases and the development of a general force field. *J. Phys. Chem. B* **2004**, *108*, 1255–1266.
- [49] Heinz, H.; Lin, T.-J.; Mishra, R. K.; Emami, F. S. Thermodynamically consistent force fields for the assembly of inorganic, organic, and biological nanostructures: The INTERFACE force field. *Langmuir* **2013**, *29*, 1754–1765.
- [50] Cheng, J.; Sprik, M. The electric double layer at a rutile TiO₂ water interface modelled using density functional theory based molecular dynamics simulation. *J. Phys: Condens. Matter* **2014**, *26*, 244108.
- [51] Ulman, K.; Poli, E.; Seriani, N.; Piccinin, S.; Gebauer, R. Understanding the electrochemical double layer at the hematite/water interface: A first principles molecular dynamics study. *J. Chem. Phys.* **2019**, *150*, 041707.
- [52] Zhang, C.; Hutter, J.; Sprik, M. Coupling of surface chemistry and electric double layer at TiO₂ electrochemical interfaces. *J. Phys. Chem. Lett.* **2019**, *10*, 3871–3876.
- [53] Jia, M.; Zhang, C.; Cheng, J. Origin of Asymmetric Electric Double Layers at Electrified Oxide/Electrolyte Interfaces. *J. Phys. Chem. Lett.* **2021**, *12*, 4616–4622.
- [54] Zhang, C.; Sayer, T.; Hutter, J.; Sprik, M. Modelling electrochemical systems with finite field molecular dynamics. *J. Phys: Energy* **2020**, *2*, 032005.
- [55] Stengel, M.; Spaldin, N. A.; Vanderbilt, D. Electric displacement as the fundamental variable in electronic-structure calculations. *Nat. Phys.* **2009**, *5*, 304–308.

- [56] Zhang, C.; Sprik, M. Finite field methods for the supercell modeling of charged insulator/electrolyte interfaces. *Phys. Rev. B* **2016**, *94*, 245309.
- [57] Jia, M.; Zhang, C.; Cox, S. J.; Sprik, M.; Cheng, J. Computing surface acidity constants of proton hopping groups from density functional theory-based molecular dynamics: Application to the SnO₂ (110)/H₂O interface. *J. Chem. Theory Comput.* **2020**, *16*, 6520–6527.
- [58] Freund, H.-J. Introductory lecture: Oxide surfaces. *Faraday Disc.* **1999**, *114*, 1–31.
- [59] Jupille, J.; Thornton, G. *Defects at oxide surfaces*; Springer, 2015.
- [60] Diebold, U. Perspective: A controversial benchmark system for water-oxide interfaces: H₂O/TiO₂(110). *J. Chem. Phys.* **2017**, *147*, 040901 – 4.
- [61] Hussain, H.; Tocci, G.; Woolcot, T.; Torrelles, X.; Pang, C. L.; Humphrey, D. S.; Yim, C. M.; Grinter, D. C.; Cabailh, G.; Bikondoa, O.; Lindsay, R.; Zegenhagen, J.; Michaelides, A.; Thornton, G. Structure of a model TiO₂ photocatalytic interface. *Nat. Mater.* **2016**, 1 – 7.
- [62] Ricci, M.; Spijker, P.; Stellacci, F.; Molinari, J.-F.; Voitchovsky, K. Direct visualization of single ions in the Stern layer of calcite. *Langmuir* **2013**, *29*, 2207–2216.
- [63] Balajka, J.; Pavelec, J.; Komora, M.; Schmid, M.; Diebold, U. Apparatus for dosing liquid water in ultrahigh vacuum. *Rev. Sci. Instrum.* **2018**, *89*, 083906 – 7.
- [64] Joutsuka, T.; Hirano, T.; Sprik, M.; Morita, A. Effects of third-order susceptibility in sum frequency generation spectra: a molecular dynamics study in liquid water. *Phys. Chem. Chem. Phys.* **2018**, *20*, 3040 – 3053.
- [65] Pezzotti, S.; Galimberti, D. R.; Shen, Y. R.; Gageot, M.-P. Structural definition of the BIL and DL: a new universal methodology to rationalize non-linear $\chi^{(2)}(\omega)$ SFG signals at charged interfaces, including $\chi^{(3)}(\omega)$ contributions. *Phys. Chem. Chem. Phys.* **2018**, *20*, 5190–5199.

- [66] Shao, Y.; Knijff, L.; Dietrich, F. M.; Hermansson, K.; Zhang, C. Modelling bulk electrolytes and electrolyte interfaces with atomistic machine learning. *Batteries & Supercaps* **2021**, *4*, 585 – 595.
- [67] Jia, W.; Wang, H.; Chen, M.; Lu, D.; Lin, L.; Car, R.; Weinan, E.; Zhang, L. Pushing the Limit of Molecular Dynamics with Ab initio Accuracy to 100 Million Atoms with Machine Learning. SC20: International Conference for High Performance Computing, Networking, Storage and Analysis. 2020; pp 1–14.